T 43
36TI

TECHNOLOGY

NATIONAL BUREAU OF STANDARDS

Technical News

BULLETIN

PUB ARY
MAY 11 1961

VOLUME 45 APRIL 1961 NUMBER 4

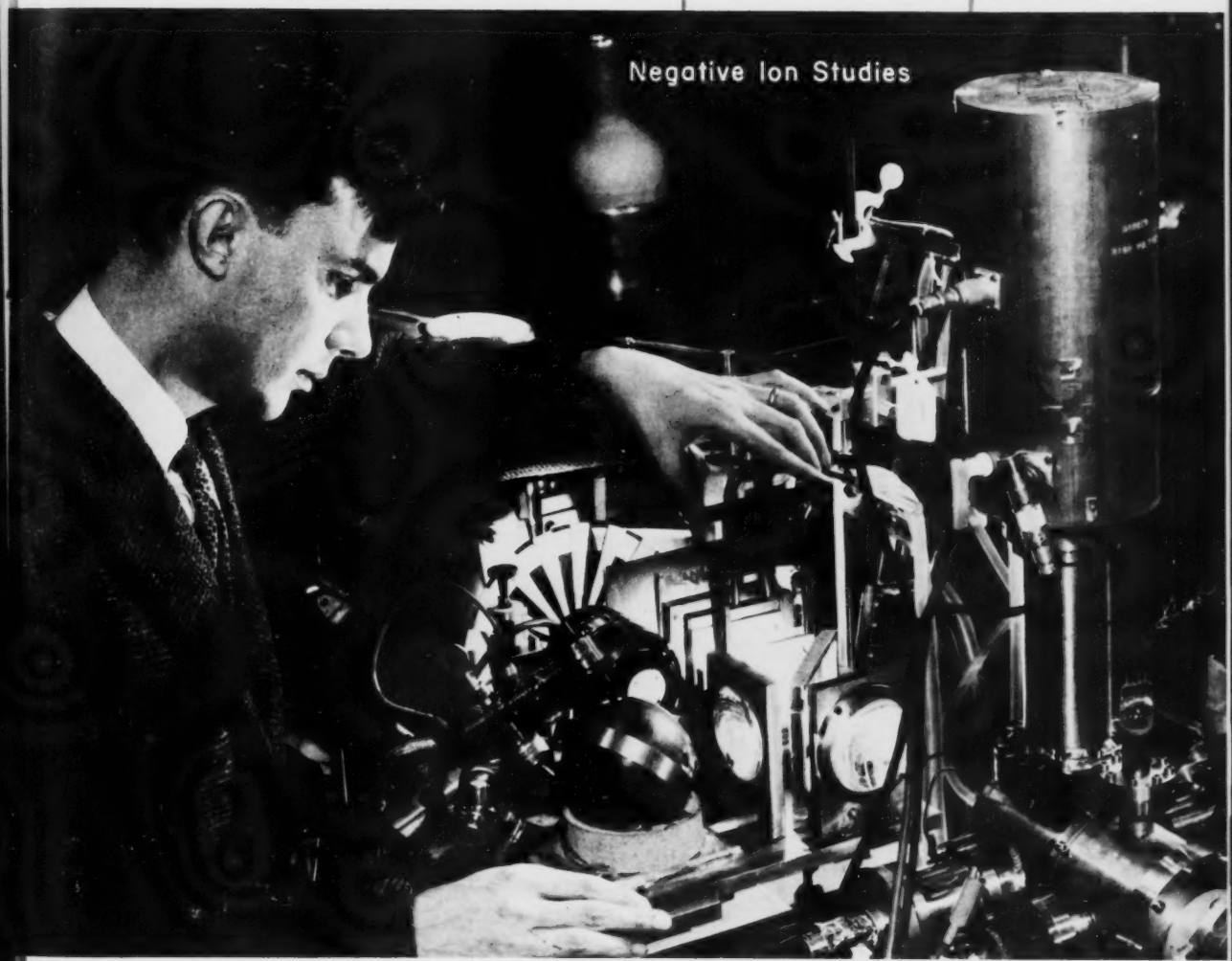

Calibration of Platinum Resistance Thermometers . . . p. 62

U.S. DEPARTMENT OF COMMERCE — LUTHER H. HODGES, *Secretary*

NATIONAL BUREAU OF STANDARDS — A. V. ASTIN, *Director*

NATIONAL BUREAU OF STANDARDS
Technical News
BULLETIN

For sale by the Superintendent of Documents, U.S. Government Printing Office, Washington 25, D.C. Subscription price, domestic $1.50 a year; 75 cents additional for foreign mailing; single copy, 15 cents. Use of funds for printing this publication approved by the Director of the Bureau of the Budget (June 24, 1958).

April 1961 — Issued Monthly — Vol. 45, No. 4

Contents

	Page
Negative Ion Studies	55
Optical Study of Supersonic Boundary-Layer Transition	57
Ephi—A Radio System for Investigating Sferics	60
Low-Temperature Reaction in Copper-Oxygen System	61
Calibration of Platinum Resistance Thermometers	62
The International Practical Temperature Scale	65
X-Ray Barrier Determinations	66
Hydrogen Bonding in Hydroxyapatites	67
Problem of Windstorm Damage to Asphalt Shingles	68
Measuring Resolving Power in Precision Lenses	70
Publications of the National Bureau of Standards	71

COVER: Part of the apparatus developed at the National Bureau of Standards for studying the photodetachment of electrons from negative atomic and molecular ions. The studies have direct bearing on ionospheric theory and research and on the study of plasmas. Dr. L. M. Branscomb inserts a filter into the optical system. See "Negative Ion Studies," opposite page.

NEGATIVE ION STUDIES

THE BUREAU has been conducting studies of the photodetachment of electrons from negative atomic and molecular ions [1] in an investigation sponsored by the Office of Naval Research. Direct interest has centered on the cross sections of negative atomic hydrogen ions and negative atomic and molecular oxygen ions because of their geophysical and astrophysical importance, although other ions having significant applications have been studied.

Theories of the ionosphere must take into account the possible diurnal variations in electron and ion densities, which may depend on the competition between the formation of negative ions by attachment of electrons and the destruction of negative ions by photodetachment. The processes of formation and destruction of negative ions must also be considered in any thermodynamic treatment of systems involving very hot gases, for electrons can become attached to some of these gases to form negative ions. For example, solar emissivity in the visible spectrum is controlled by the hydrogen ion through bound-free transitions.

Information obtained on the continuous solar spectrum in the region between 0.6 and 1.6 μ shows departures from the Planck curve characteristic of a blackbody. These departures were first ascribed, by R. Wildt at Yale in 1939, to the continuous absorption of the negative hydrogen ions in the solar photosphere.[2] In 1950 W. L. Fite at Harvard attempted to detect photodetachment from the negative hydrogen ion. Although his experiment was not successful, it led to the development of the high-current negative ion source now in use at the Bureau and helped determine the present experimental approach to the problem.

The experimental study of photodetachment of electrons from negative ions, a special case of photoelectric absorption, originated in 1953 [3] when L. M. Branscomb, of the Bureau staff, and W. L. Fite, a consultant to the Bureau, made the first laboratory observation of the process

$$H^- + h\nu \rightarrow H + e.$$

A small current of free electrons produced in high vacuum by photon absorption at the intersection of two mutually perpendicular beams, one of negative ions and the other of intense visible light, was collected and measured. In 1954 and 1955, measurements of photodetachment cross sections for negative ions of several gases [4] were made at the Bureau by L. M. Branscomb and S. J. Smith using the same crossed-beam geometry and very simple ion and photon sources and optics.[5]

This high-vacuum crossed-beam apparatus, developed by the Bureau for the study of photodetachment of electrons from negative ions, has recently been improved.[6] The refinements by Smith and Branscomb have made possible a very accurate measurement of the electron affinity of atomic oxygen [7] and reliable point-by-point measurements of the spectral dependencies of the photodetachment cross sections for negative atomic hydrogen ions and negative atomic and molecular oxygen ions.[8]

The improvement of this crossed-beam apparatus has included the development of (1) an optical system which permits the use of sets of filters to obtain quasi-monochromatic light; (2) a mass spectrometer having a high-transmission magnetic sector field to ensure the purity of the ion beam; and (3) an a-c preamplifier, amplifier, and synchronous detector which permit detection of the photodetached electrons with very high sensitivity. The choice of the instrumentation involved a difficult search for a workable compromise in meeting simultaneous requirements for resolution and intensity in both the ion beam and the photon beam, under severe limitations imposed by available detection sensitivity.

A single ion passing through the photon beam has its extra electron photodetached with a probability dependent upon the photodetachment cross section and the photon flux density along the path of the ion. Cross sections successfully measured have ranged from about 4×10^{-17} cm^2 at the maximum for H^- down to about 5×10^{-20} cm^2 near the threshold for O_2^-. These limits correspond to photodetachment probabilities ranging from about 10^{-5} to about 1.5×10^{-7} per watt/cm^2 per cm of ion path, assuming ion velocities corresponding to 300 ev of energy. Actual photon beam intensities were of the order of $\frac{1}{4}$ v.

The photodetachment process is in competition with the detachment of electrons by collisions with the background gas. The Bureau's experiments were conducted at pressures of the order of 10^{-6} mm Hg, for which the collisional detachment probability is roughly 2×10^{-5}/cm of path,[9] yielding a current of free electrons which is larger than that produced by photodetachment. The photodetachment signal is separated from the collisional detachment background by modulation of the photon beam at 450 c/s and measurement of that component of the free electron current which alternates synchronously with the modulated photon beam. Ideally, the photodetached electron current yields an a–c signal having the same waveform as the chopped light, while the collisionally detached electron current yields a d–c signal. A measurement of the a–c component of the detached electron current using appropriate filter networks to eliminate the d–c component is therefore a measurement of the photodetachment current.

The electrons detached in the reaction chamber at the crossing of ion and photon beams are separated from the ions and trapped by weak magnetic and electric fields. They are then collected on a metal cap which connects directly into the grid circuit of a very-high-impedance preamplifier.

The ions studied thus far by the photodetachment method are H^-, O^-, O_2^-, OH^-, OD^-, and S^-,[10] which, in addition to possessing interesting applications, can be produced relatively easily as anode rays from a low-pressure discharge in the quantities required. In addi-

tion, they are low-mass ions, which simplifies the problem of mass resolution. The study of less easily produced and analyzed ions is the next objective of the photodetachment program.

[1] *L. M. Branscomb and S. J. Smith, Phys. Rev.* **98,** *No. 4, 1028 (1955); S. J. Smith and D. S. Burch, Phys. Rev. Letters* **2,** *No. 4, 165 (1959); S. J. Smith and D. S. Burch, Phys. Rev.* **116,** *No. 5, 1125 (1959).*

[2] *R. Wildt, Astrophys. J.* **89,** *295 (1939).*

[3] *L. M. Branscomb and W. L. Fite, Phys. Rev.* **93,** *651 A (1954).*

[4] *L. M. Branscomb and S. J. Smith, Phys. Rev.* **98,** *1028 (1955); Phys. Rev.* **98,** *1127 (1955).*

[5] *S. J. Smith and L. M. Branscomb, J. Research NBS* **55,** *165 (1955).*

[6] *For further information, see* Optical methods for negative ion studies, *by Stephen J. Smith and Lewis M. Branscomb, Rev. Sci. Inst.* **31,** *No. 7, pp. 733–747 (1960).*

[7] *L. M. Branscomb, D. S. Burch, S. J. Smith, and S. Geltman, Phys. Rev.* **111,** *504 (1958).*

[8] *S. J. Smith, Proc. Fourth Internatl. Conf. Ion. Phenom. in Gases; D. S. Burch, S. J. Smith, and L. M. Branscomb, Phys. Rev.* **112,** *171 (1958); S. J. Smith and D. S. Burch, Phys. Rev. Letters* **2,** *165 (1959); Phys. Rev.* **116,** *1125 (1959).*

[9] *J. B. Hasted, Proc. Ray. Soc. (London)* **[A] 212,** *235 (1952).*

[10] *See footnotes 2–5; also, L. M. Branscomb and S. J. Smith, J. Chem. Phys.* **25,** *598 (1956); S. J. Smith and L. M. Branscomb, Bul. Am. Phys. Soc. Ser. I,* **30,** *31 (1955).*

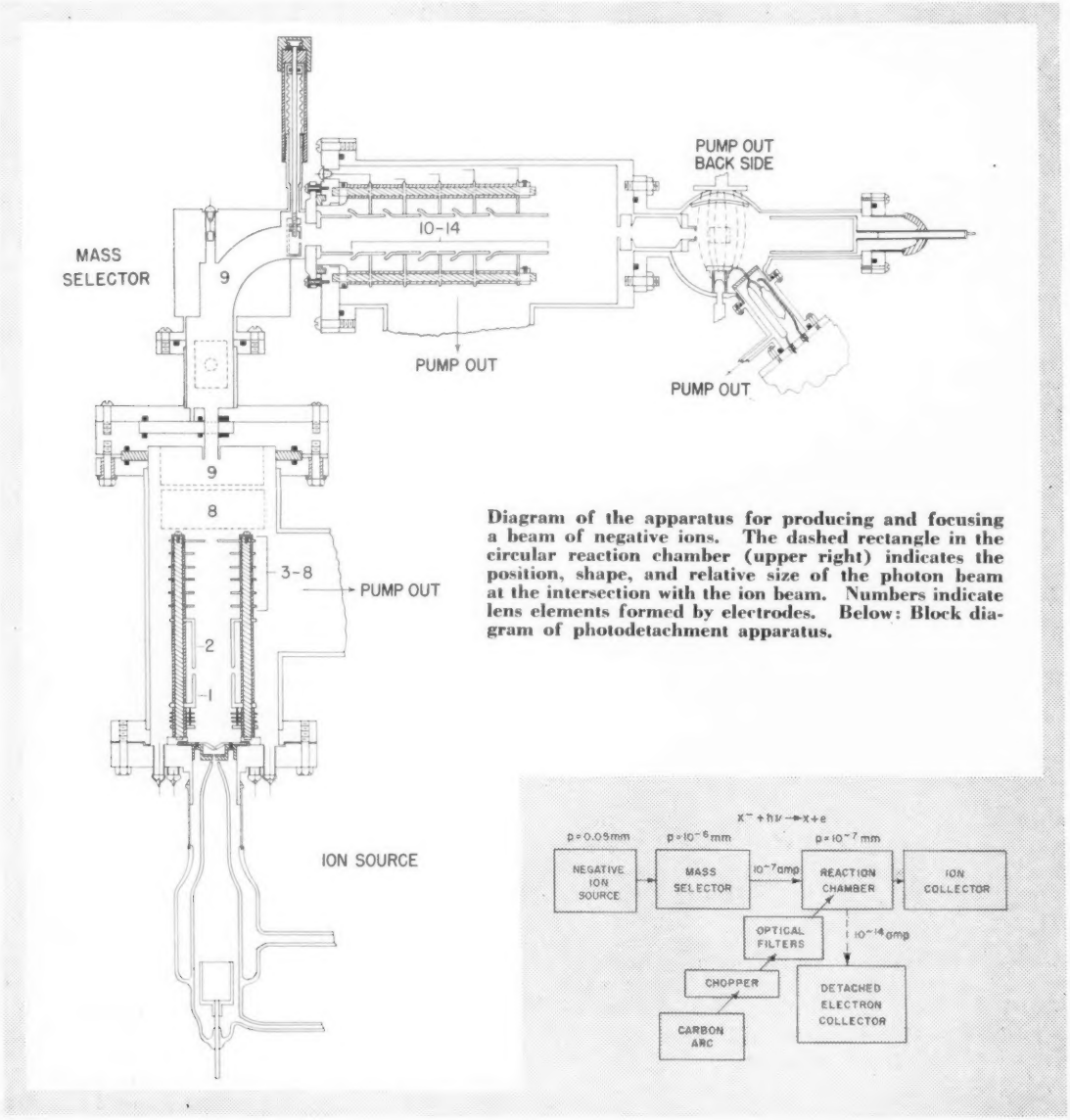

Diagram of the apparatus for producing and focusing a beam of negative ions. The dashed rectangle in the circular reaction chamber (upper right) indicates the position, shape, and relative size of the photon beam at the intersection with the ion beam. Numbers indicate lens elements formed by electrodes. Below: Block diagram of photodetachment apparatus.

Optical Study of Supersonic Boundary-Layer Transition

AN OPTICAL STUDY of the boundary-layer transition processes in a supersonic air stream [1] has been made by W. G. Spangenberg and W. R. Rowland of the Bureau in work sponsored by the National Aeronautics and Space Administration. The aerodynamic boundary layer is the portion of air immediately contiguous to an object in an air stream. In the boundary-layer region, the velocity of the stream is affected by the presence of the object, and the frictional qualities of the air are important in determining the air flow.

In most instances of fluid flow near a smooth wall, such as the outer surface of a missile, the flow is laminar for some distance from the leading edge and then becomes turbulent because of instabilities resulting from variations in velocity throughout the boundary layer. This change of regime, called transition, increases the rate of transfer of properties such as momentum and aerodynamic heating between the wall and the stream, causing increased skin friction at all speeds and significantly increased wall temperatures at higher speeds where aerodynamic heating becomes important.

A better understanding of the physical role played by transition processes in boundary-layer behavior would aid in the design of longer-range, higher-speed aircraft and missiles. Some designs of re-entry vehicles also must take into account the heating effects of boundary layers.

Microsecond-exposure sequential schlieren photographs of transition areas taken during the Bureau's study provide definite optical evidence that the boundary-layer transition processes in a supersonic air stream are similar to those in a subsonic stream. The photographs were taken with an unusual cylindrical-lens camera [2] designed by Mr. Spangenberg.

Transition has been studied extensively under various conditions, but the processes leading to it have been revealed only in part. Most investigations of transition phenomena have been conducted using hot-wire anemometers at low speeds where air can be regarded as incompressible and frictional heating effects neglected. The extension of their use to supersonic flow has been limited. Previous experiments [3] have established that in the absence of naturally large disturbances transition is initiated by the self-amplification of the small disturbances within the stream.

The localized breakdown of these disturbed regions and the subsequent growth of turbulent "spots" so clearly evident from observations at low speeds [4] have been observed sporadically at supersonic speeds, but have never been recognized as an inherent part of the transition process. The purpose of the Bureau's study was to obtain detailed information on the history of transition from laminar to turbulent flow in the boundary layer on a hollow cylindrical model in a supersonic air stream to learn whether the processes occurring at supersonic speeds are similar to those observed in low-speed flow. A particular objective of the investigation was to find whether there is any correlation between local breakdown of laminar flow to turbulent spots and the transition process.

Since use of the hot-wire anemometer in supersonic and transonic air streams [5] involved extreme difficulties, schlieren photography was utilized to determine the nature of the transition region with the hope of possibly correlating these observations with hot-wire information in the future to obtain a more detailed description of transition phenomena.

Optical System

A schlieren system can be used to view the variations in refractive index within a boundary layer which are associated with differences in frictional heating. At all supersonic speeds, these variations are sufficient to supply information pertinent to transition—a transient process of short duration.

In schlieren photographs taken with the cylindrical-lens camera, the image of the viewed area is recorded three times full size in the vertical dimension and 3/20 full size in the 6-in. horizontal dimension. The mag-

Supersonic wind tunnel showing part of the schlieren optical system. W. R. Rowland monitors the oscillator signal on the oscilloscope. The test section with a hollow cylindrical model in place is in the upper foreground; behind it can be seen the cylindrical-lens camera assembly (rotating-mirror camera is above it but hidden by the tunnel) and (further back) the standard camera.

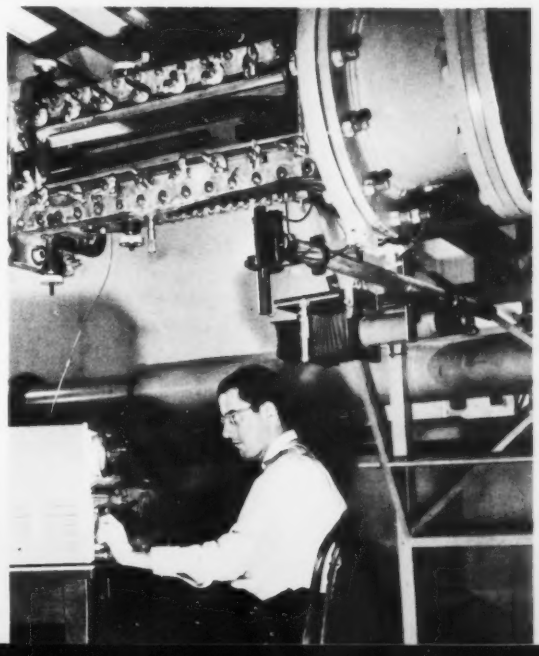

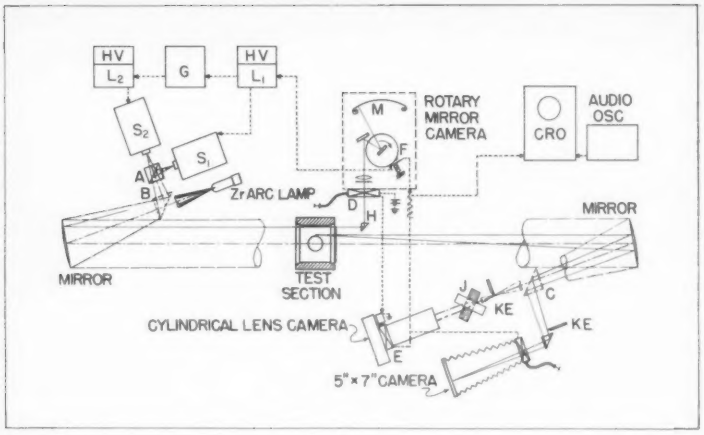

Diagram of optical system and controls. Motor speed of the rotating-mirror camera is adjusted to be synchronous with the signal from the audio oscillator as monitored on the cathode-ray oscilloscope. Shutter E of the cylindrical-lens camera is opened magnetically when camera shutter D is opened manually, causing an electrical contact within E to close. When the commutator F in the rotating-mirror camera makes contact, the thyratron circuit L_1 fires the spark source S_1. After a period determined by the delay circuit G, S_2 is fired by L_2. The rotating-mirror camera records the exact time delay by sweeping images of light obtained through prism H from S_1 and S_2 onto film strip M. Light pulses from sources S_1 and S_2 enter the system through beam-splitting prism A. Selection of spark source or continuous arc source is made through prism B; camera is selected with prism C. J is a light-refracting arrangement that allows the two sequential photographs to be taken on one film frame.

nification ratio of the depth of the extremely thin boundary layer to its length permits close inspection of the areas of turbulent "spot" eruption and of their movements as shown by sequential photographs. The particular values of magnification were so chosen that the lens can be used with a standard camera. All the elements of the camera lens except the condensing mirror of the schlieren system are contained within a tube 2¼ in. in diameter and about 4 ft in length to make it easily adjustable.

Both flash and continuous light sources are provided. The schlieren image obtained using either source may be recorded by either a standard camera or with a 20:1 magnification ratio by the cylindrical-lens camera. The light source and the camera are selected through the use of auxiliary prisms.

The spark light source for the flash photographs is installed in duplicate so that two independent pictures of the test section may be taken in rapid sequence. Knowing the time delay (as measured with a rotating-mirror camera designed by the Bureau) between two sequential photographs, one can compute the velocity, growth rate, and frequency of turbulent spots. The continuous arc light source and the standard camera aid in visual examination of the transition region.

The effect of refraction of light passing through the boundary layers on the test section windows is prominent in spark photographs taken with a standard camera-lens combination and detracts from their quality. Direct photography of the boundary layer on the test body with the cylindrical-lens camera produces pictures that are not so adversely affected by this refraction because the depth of focus of this lens in the magnified plane is only a small fraction of the width of the tunnel.

Experimental Conditions

The study was made in the supersonic wind tunnel, which has a 3- by 4-in. fixed test section, at a Mach number of 1.96. The stagnation pressure of the continuously operating variable-density tunnel may be varied from 0.1 to 3.0 atm (corresponding to Reynolds numbers per inch from 0.03×10^6 to 1×10^6), and the stagnation temperature, from 80 to 140 °F.

Hollow steel cylinders and cone-cylinder combinations of varying diameter were used as models. Most observations were made using a hollow cylinder of hardened steel having an outside diameter of 1¼ in. and a thickness of 0.015 in., with a sharp leading edge. Its surface was ground and polished to a residual roughness of 3 to 4 μin. (arithmetic average). For some of the tests, a small area of roughness was added near the leading edge of the cylinder to generate turbulent spots.

Results

Results of the study show that transition in a supersonic stream starts with high-frequency disturbances in the laminar boundary layer which degenerate into areas of turbulent flow. These "spots" of turbulence erupt independently near the trailing face of the turbulent flow region, which is constantly moving downstream. The addition of newly turbulent areas of finite size to the trailing face of the region causes it to jump upstream discontinuously. These spots are traveling at about 0.25 to 0.5 free-stream velocity at the time that they first become visible, and as they continue downstream accelerate to a velocity about 0.7 free-stream speed at their trailing face.

The origin of fresh areas of breakdown to turbulence apparently is in amplified Tollmein-Schlichting waves. Turbulent spots are most frequently produced within the region in which one can predict, using stability theory, that disturbances within the boundary layer will be amplified. It can be concluded from these results that transition mechanisms in supersonic flow are similar to those in a subsonic air stream.

[1] An optical study of the boundary layer transition processes in a supersonic air stream, *by W. G. Spangenberg and W. R. Rowland, Phys. of Fluids* **3**, *No. 5, 667–684 (1960)*.

[5] *The basis for this design is given in* Lens system producing unequal magnification in two mutually perpendicular directions, *by Donald R. Buchele and Herman R. Goossens Rev. Sci. Instr.* **25**, *No. 3, 262–263 (1954)*.

[3] Laminar-boundary-layer oscillations and transition on a flat plate, *by G. B. Schubauer and H. K. Skramstad, NACA Rep. 909 (1948)*; Stability of a supersonic laminar boundary layer on a flat plate, *by J. Laufer and T. Vrebalovich, Jet Prop. Lab., Cal. Inst. Tech., Rep. 20–116 (1958)*.

[4] Contributions on the mechanics of boundary-layer transition, *by G. B. Schubauer and P. S. Klebanoff, NACA TN 3489 (1955)*; Evolution of amplified waves leading to transition in a boundary layer with zero pressure gradient, *by P. S. Klebanoff and K. D. Tidstrom, NASA TN D–195 (1959)*.

[2] Turbulence in supersonic flow, *by L. S. G. Kovasznay, J. Aero. Sci.* **20**, *No. 10, 657–674 (Oct. 1953)*; Heat-loss characteristics of hot-wire anemometers at various densities in transonic and supersonic flow, *by W. G. Spangenberg, NACA TN 3381 (1955)*; Fluctuations and hot-wire anemometry in compressible flows, *by M. V. Morkovin, AGARDograph 24, NATO Adv. Group for Aero. Research (Paris, 1956)*.

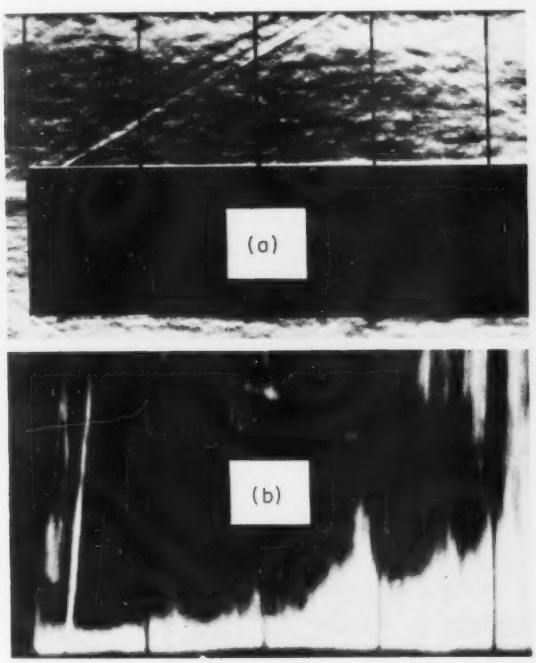

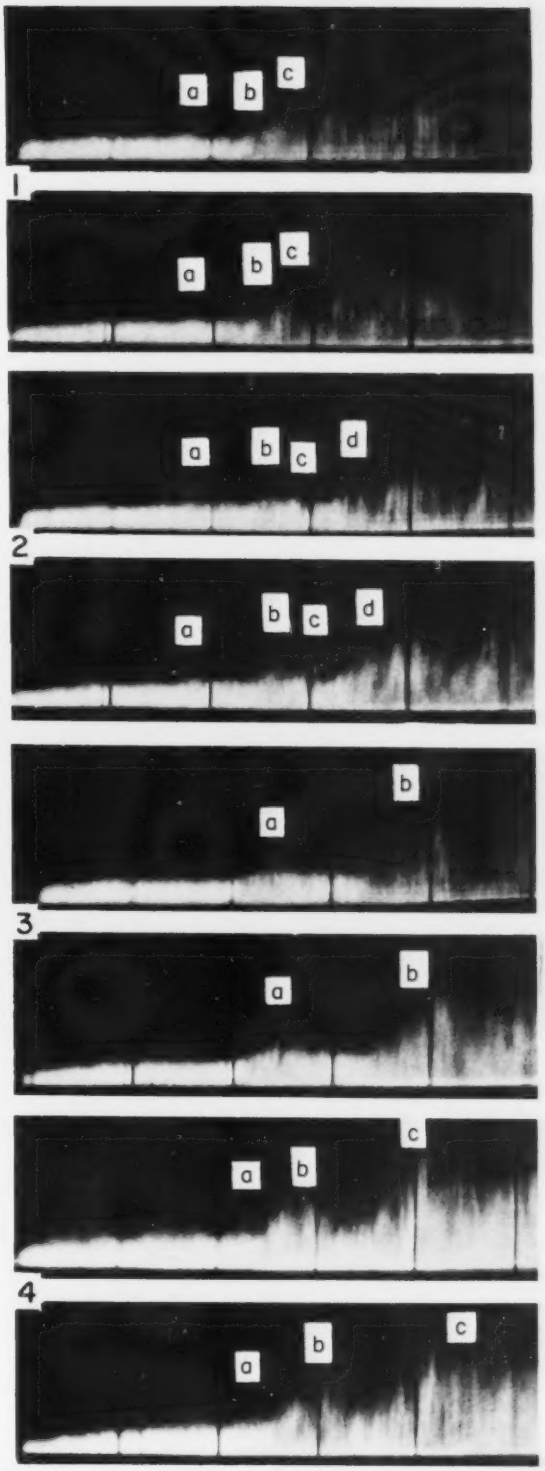

Above: Photographs illustrate the effectiveness of the cylindrical-lens camera in defining the boundary layer in the transition region. (a) Spark schlieren photograph of boundary-layer transition region taken with standard camera. (b) Photographic copy of boundary layer of (a) made with 20:1 magnification cylindrical-lens camera. Vertical lines are 1 inch apart. The object in the air stream is a hollow cylinder, 1¼ in. diam, with roughness element near leading edge; Reynolds no./in., 0.61×10^6. (Flow from left to right.) Right: Sequential spark schlieren photographs showing steps in development of a turbulent spot. In each pair of pictures the upper picture was taken first and the lower picture at a measured time later. (Time delay between the upper and lower pictures of the first 3 pairs is 3.2 μsec; that between the fourth pair 6.8 μsec.) There is no time correlation among the four pairs. Smooth model; Reynolds no./in., 0.62×10^6.

Ephi—A Radio System for Investigating Sferics

A VERSATILE TECHNIQUE for investigating electromagnetic waves originating from lightning discharges ("sferics") has been developed by the Boulder Laboratories. "Ephi," the name for this new system which locates and analyzes sferics, is capable of appreciably greater accuracy than direction-finding systems that have been used in the past.

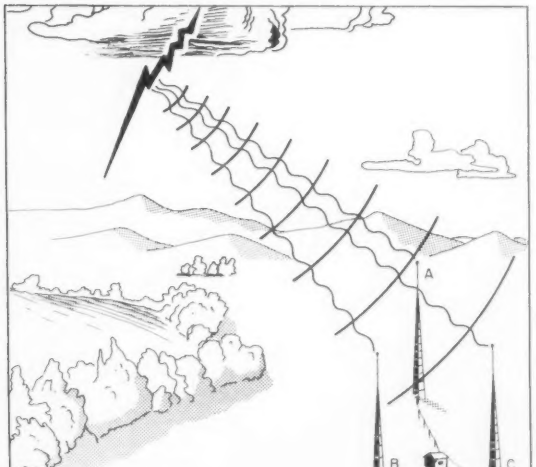

Antenna system of Ephi consists of three 125-ft towers spaced about 4 miles apart, forming the vertices of an equilateral triangle. The signals received at each antenna are fed over coaxial cables to the central control station of the system.

The experimental equipment for the Ephi system has been installed near Brighton, Colo., by the Navigation Systems Section of the Radio Systems Division. The system was developed by G. Hefley, R. F. Linfield, T. L. Davis, and R. H. Doherty.[1]

The antenna system consists of three 125-ft towers spaced about 4 mi apart, forming the vertices of an equilateral triangle. The signals received at each antenna are fed over coaxial cables to the central control station of the system. Here electronic equipment determines the relative difference in time of arrival of the sferic signal from each antenna, and, from this, the direction from the control station to the lightning source is automatically determined.

Since sferics travel with the speed of light and the antennas are so closely spaced, the differences in time of arrival at the three antennas are so small that they are measured in microseconds. The maximum difference in arrival time between the antennas at Brighton is only about 21 μsec. The Ephi equipment can make such measurements of time difference with an accuracy of a small fraction of a microsecond.

In addition to determining the direction of arrival of sferic signals, the equipment counts the total number of sferics occurring in any desired time interval, and can count the number of sferics arriving from several different directions at the same time. The sferic waveform can also be photographed, either with still or motion-picture cameras, and the record retained for further detailed studies aimed at a better understanding of radio wave propagation as well as the nature of the lightning itself.

In addition to its value as a research tool, "Ephi" is potentially of value in tracking such severe weather

Charles A. Samson checks the electronic equipment used to determine the relative difference in time of arrival of the sferic signal from each antenna. From this, the direction from the station to the lightning source is automatically determined.

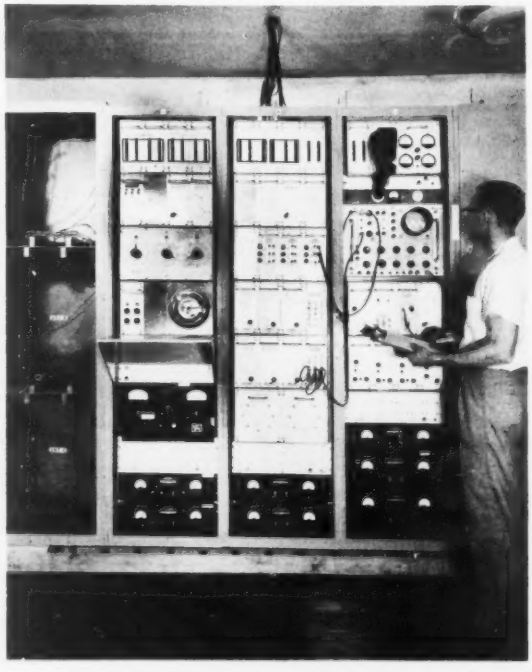

phenomena as tornados and hurricanes. These storms are usually accompanied by sferics of high intensity which can be detected by the equipment.

The Ephi station at Brighton can pick up sferic signals originating in storms far offshore in the Gulf of Mexico or the Atlantic Ocean. Two such stations, located a few hundred miles apart, could accurately "fix" the position of a storm at distances of many hundred of miles from either station.

[1] *For further technical details, see* The Ephi system for VLF direction finding, *by G. Hefley, R. F. Linfield, and T. L. Davis, J. Research NBS,* **65C,** *43 (1961).*

Low-Temperature Reaction in Copper-Oxygen Systems

AN INTERESTING PHENOMENON was observed during the recent free radicals research program which the Bureau conducted for the Department of Defense.[1] In experiments performed by Jerome Kruger and William Ambs of the corrosion laboratory, no reaction occurred when oxygen was deposited at a temperature of 4 °K on the surface of a copper specimen. But when the oxygen was partially dissociated by passage through a high-frequency microwave discharge before a similar deposition, a thin film formed that remained solid at room temperature.[2] These results—of particular significance to work on the fundamental mechanisms of corrosion—will be the basis for further research on other metals and gases.

In recent years numerous investigations have been carried out on short-lived reactive species first formed in an electric discharge and then trapped and stored on a low-temperature surface. However, a few data have been made available on the reactions occurring between oxygen and a metal surface at very low temperatures. The present work was therefore initiated to complement the free radicals program, and copper was chosen as the metal surface to be studied because of its known chemical properties.

Both single-crystal and polycrystalline specimens of 99.99 percent copper were used in the study. Their surfaces were specially prepared to make them clean, strain-free, and smooth. The experiments were carried out under closely controlled conditions in which Dewar pressure during deposition was 2×10^{-5} mm of mercury, and inlet pressure of the oxygen was 0.15 to 0.7 mm of mercury. In these experiments, molecular oxygen was found to have no effect at any temperature from 4 °K up to 300 °K. However, when the oxygen was passed through the discharge and the copper surface was held at 4 °K during deposition, a film of reaction product about 20 A thick formed. The film on all of the surfaces studied ([100], [110], and [111]) was of the same thickness, and it did not increase in subsequent runs. Since no film was found on a gold surface employed as a control, it appears that no extraneous material was deposited. The thickness of all the films found was determined by means of an ellipsometer.

The discharged oxygen had no effect on copper specimens at 40 °K or higher. Further, if a thin film of molecular oxygen was placed on the surface and discharged oxygen condensed on top, no reaction was observed. It therefore seems that the solid film deposited under controlled conditions is due to atomic oxygen, and that the reaction product may be an oxide. The formation of the film was probably caused by a reaction between the condensed oxygen and the copper surface, with the activation energy being provided by recombinations of oxygen atoms.

[1] Stabilization of free radicals at low temperatures, *NBS Mono. 12 (1960), available from the Superintendent of Documents, U.S. Government Printing Office, Washington 25, D.C. ($1.50)*; Results of free radicals research, *NBS Tech. News Bul.* **44,** *100 (1960).*

[2] *For further details, see* Reaction between copper and solid oxygen condensed at very low temperatures from a gas discharge, *by Jerome Kruger and William Ambs, Nature* **186,** *794 (1960).*

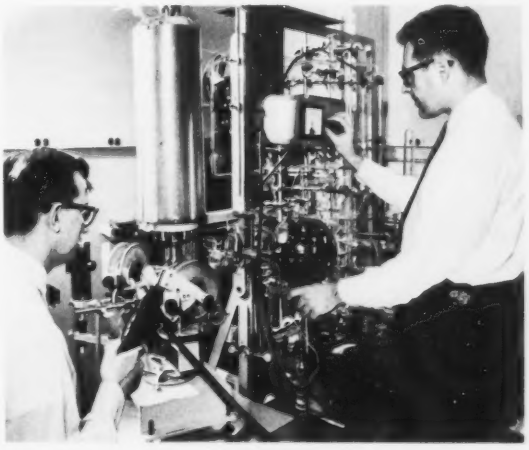

Equipment used to condense gases on metals at low temperatures. Dr. Jerome Kruger (right) adjusts the pressure of oxygen being introduced into a high-frequency microwave discharge as William Ambs initiates the discharge with a Tesla coil. After passing through the discharge, the oxygen condenses on a copper specimen inside the lower part of the Dewar assembly (upper left). The ellipsometer in front of Mr. Ambs is used to observe and measure the thickness of the film that forms on the specimen.

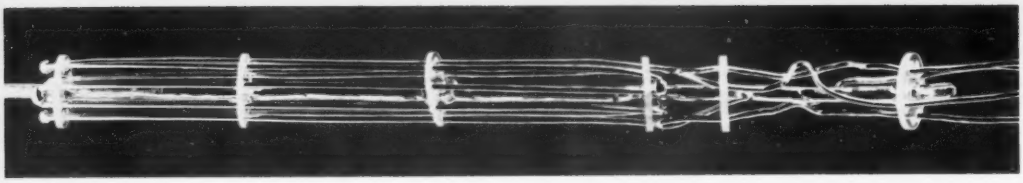

Calibr

third a se

THERE IS a growing need in all branches of science and technology for temperature measurements of increased accuracy and precision. This is true not only over the usual range of temperatures, but in the more extreme temperature regions as well. Platinum resistance thermometers, which can be used over a wide range of temperatures with great effectiveness, help to fill this need. The Bureau, through its calibration services, contributes to the accuracy and uniformity of temperature determinations made with these instruments.

Although there are many types of resistance thermometers, employing a variety of materials, the Bureau specifies that only thermometers having a four-lead resistor of very pure platium, hermetically sealed in a protecting tube, be submitted for calibration.[1] Resistance thermometers are made in three general forms: long-stem, capsule, and calorimetric. The sensing element in the long-stem and capsule types consists of a fine helix of platium wire wound bifilarly on a supporting frame of mica. The winding is supported by notches in the mica frame in such a manner as to leave the wire as strainfree as possible. Near each free end of the coil is attached an additional short platinum lead wire, making the sensing element a four-lead resistor. The coil is protected by enclosure within a gas-filled case.

The capsule thermometer is short, about 2 in. in length, and has a platinum case. The lead wires exit through an air-tight glass seal, and the capsule is filled with a mixture of helium with 2 percent oxygen. As the entire capsule, including the glass seal, is at the temperature being measured, and because glass becomes significantly conducting at high temperatures, this type of resistance thermometer is not normally used above 300 °C.

The stem-type resistance thermometer is usually about 18 in. long, although the resistance coil is quite small. The short platinum leads of the resistor are attached to four gold extension wires, and the entire assembly is enclosed within a glass cylinder containing dry nitrogen and 2 percent oxygen. Because of the length of this device the point where the wires exit through the case is at room temperature. Therefore, stem-type thermometers are often used to 500 °C if encased in glass and to 630.5 °C and above if enclosed in quartz.

The third type of platinum resistance thermometer, used in calorimetric measurements, has a coil wound on a flat strip of mica which is encased within a thin metal sheath. The case is filled with dry air. This type of construction has a more rapid thermal response, which is an advantage for some types of calorimetric determinations.

High-temperature platinum resistance thermometer developed by the Bureau has platinum wire threaded through disk supports made of synthetic sapphire. This device has been found to drift as little as 0.001°/hr. at 1,000 °C.

Capsule-type resistance thermometers are calibrated at temperatures as low as 10 °K (−263 °C) but, because of the electrical conductivity of the glass at high temperature, they are usually not calibrated at the sulfur point. Thermometers of the stem type are calibrated at the boiling points of oxygen (−182.97 °C), water, and sulfur (444.6 °C), and at the triple point of water (0.01 °C), and those of the calorimetric type are calibrated at the triple point, steam point, and near 50 °C. The capsule- and stem-type thermometers are annealed before calibration by being placed in the re-entrant wells of the sulfur boiler for 4 hr.

A. B. Castle, Jr. makes sure that there is a water-ice interface completely surrounding the re-entrant well of a triple point cell. This cell is used to attain a defining fixed point (0.01 °C) on the International Practical Temperature Scale for the calibration of platinum resistance thermometers.

...libration of Platinum Resistance Thermometers

...third a series on NBS measurement and calibration services

Resistance Measurement

The resistance of the thermometer being calibrated is measured with a Mueller-type bridge. Readings are taken to the nearest 10 μohms, with a current of 2 ma flowing in the thermometer. In most cases, the heating effect of this current can be ignored if the thermometer is used with this same current. However, if the thermometer is to be used under conditions where the thermal contact is poor or variable, errors which might arise from the heating effect can be minimized if all (calibration and actual use) resistance readings are taken with both 2 and 5 ma flowing in the thermometer, and the resistance at zero current found by extrapolation. To eliminate the resistance of the lead wires attached to the platinum resistor, readings are made with two combinations of bridge-lead connections. The resistance of the coil alone is then the average of the two readings.

Low-Temperature Calibration

Over the range of 10 to 90 °K, capsule type resistance thermometers are calibrated in a hydrogen bath against one of the standard resistance thermometers maintained by the Bureau. Both the test and standard thermometers are inserted into a copper block, and the necessary connections are made. This aggregate is then placed within the cryostat. The system is sealed from the atmosphere by soldering an airtight canister to the stationary cover with Woods metal. The temperature within the cryostat is controlled at temperatures below 20 °K by adjusting the pressure on the liquid hydrogen refrigerant within the cryostat. At temperatures above 20 °K, the temperature is controlled by electrically heating the block to achieve the desired temperature and then heating the shield to maintain this temperature. A control system, actuated by a multiple-junction thermocouple between the copper block and the shield, maintains the temperature within narrow limits. After thermal equilibrium is achieved at each calibration temperature, several simultaneous resistance readings are taken on each thermometer and the standard.

A second cryostat is used for the calibration of both capsule- and stem-type resistance thermometers at the oxygen point (−182.97 °C). Once again, a comparison is made with a standard resistance thermometer. Because the thermometers are inserted in long re-entrant wells, a lead-wire assembly must be attached to capsule-type thermometers, and a glass protection tube is slipped over both the thermometer and lead wires. Liquid nitrogen is used to cool the cryostat, and a heating coil, controlled automatically as in the hydrogen bath, is used to maintain the temperature at the oxygen point. Several readings are taken for each thermometer at the oxygen point.

Triple Point Calibration

Although the triple point of water (0.01 °C) was not adopted as a defining fixed point on the International Practical Temperature Scale [2] until 1960, the Bureau has been using triple point cells in calibration activities for many years. The cell consists of a sealed glass cylinder nearly filled with pure, air-free water. A re-entrant well is provided for the insertion of a thermometer. In use, the cell is cooled by immersion in an ice bath, and a mantle of ice is formed around the re-entrant well with dry ice. After a sufficient mantle has formed it is freed from the glass by slight warming from within the well, to provide an immediately adjacent water-ice interface. The thermometer is then inserted into the well, using an aluminum bushing for good thermal contact. Resistance readings are

Basic types of platinum resistance thermometers calibrated by the Bureau. At the upper left is a metal-encased thermometer used in calorimetry. The short capsule-type thermometer (center) must be attached to the 4-lead assembly above it and inserted in the glass protection tube below it when it is to be positioned in a deep re-entrant well. A stem-type thermometer is shown at the bottom. Inset shows close-up view of the coil (about 1 in. long) of a platinum resistance thermometer. The fine platinum wire is wound on a mica support in as strain-free a manner as possible.

Above: Cryostat used in calibrating capsule-type resistance thermometers at very low temperatures. Both test and standard thermometers are inserted in the copper block (lower right) and this assembled unit is placed up into the metal Dewar immediately above. A second Dewar (center background) is positioned around the jacket and soldered to the plate near the top. The entire assembly is surrounded with liquid nitrogen. Liquid hydrogen is transferred into the inner Dewar, and the temperature is controlled over the range 10 to 90 °K by a combination of pumping on the hydrogen and heating the block. Below: Diagram of circuits used to eliminate effect of lead resistance when calibrating platinum resistance thermometers. In A three of four leads (C, c, t, T) of the thermometer are connected to the bridge; in B the connections have been reversed. By taking resistance readings in the two positions and averaging the results, the resistance of the sensing element alone can be determined.

then taken after equilibrium is achieved. To check on the stability of a thermometer during calibration, the resistance at the triple point is determined before and after measurement at any of the other fixed points.

Steam and Sulfur Point Calibration

Special boilers, operating in a closed system in which the pressure can be closely regulated, are used to reproduce the steam (100 °C) and sulfur (444.6 °C) points.[3] Helium gas is employed to transmit the pressure to a precision manometer. The boilers are cylindrical, with re-entrant wells extending from the top into the vapor region. The water boiler was constructed of copper, heavily tinned on the inside to prevent contamination, and the sulfur boiler was made of 2S aluminum. At the bottom of each boiler is a re-entrant dome, inside of which is placed an electric heater. Tangent to the dome, and within the boiler, are positioned vertical silver (water boiler) or aluminum (sulfur boiler) wires which prevent explosive boiling. Radiation shields are placed within the boilers to isolate the re-entrant wells from the boiler walls and heating zone. The vapors are condensed at the top of the boiler by means of a water-cooled jacket. The level of the helium-vapor interface, which must be known for the determination of pressure, is measured with thermocouples placed within the walls of the condenser.

The water boiler reaches thermal equilibrium quite rapidly, but experience has shown that temperature changes occur within the sulfur boiler for some time. Therefore, calibrations are not started until the sulfur has boiled for at least 10 days. With each boiler, several resistance readings are taken for each thermometer after equilibrium is reached in the re-entrant wells.

Other Services

The Bureau also calibrates calorimetric-type resistance thermometers. This calibration is accomplished by determining the resistance at the ice and

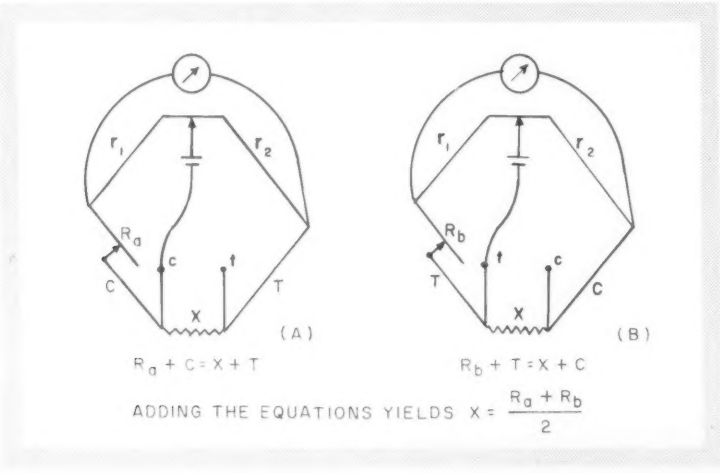

$R_a + C = X + T$ $\qquad$ $R_b + T = X + C$

ADDING THE EQUATIONS YIELDS $X = \frac{R_a + R_b}{2}$

steam points, and at a third point near 50 °C. A stirred water bath, in which the test thermometer is compared with a standard thermometer, is used for the latter point.

Also, the resistance of platinum wires such as are used in thermocouple construction is determined at the triple and steam points. The resistance at 0 °C is then computed, and the ratio of the resistances at 0 and 100° (R_{100}/R_0) is determined. This ratio must exceed 1.3920 to meet the specifications of the International Practical Temperature Scale.

Certification

Certificates containing the appropriate constants for use in the specified interpolation equations are prepared for each thermometer submitted for calibration. Separate tables, which relate resistance to temperature at 0.1° (below −183 °C) or 1.0° (above −183 °C) intervals, are also prepared. All values are derived from the raw data by a high-speed computer.

Research

Research is being conducted in several areas to extend the accuracy and range of platinum resistance thermometers. A thermometer has been constructed, consisting of platinum threaded through holes drilled in synthetic sapphire disks, and has been found to drift less than 0.001°/hr at 1,000 °C.[4] Further development of resistance thermometers for use at high temperatures may eventually lead to the extension of the defining range of these thermometers on the International Practical Temperature Scale to 1,063 °C. The present limit is 630.5 °C.

Effort is being made to put the calibration procedure on a more automatic basis. A read-out device is being incorporated to permit automatic recording of all raw data, which will facilitate communication with the computer. Plans have been made to permit the oxygen bath to be connected to the precision manometer and which will provide, directly, a defining fixed point temperature (−182.97 °C). Plans are also being made to construct an apparatus for the calibration of resistance thermometers at the zinc point (419.505 °C). This temperature, which is more reproducible than the sulfur point, has been accepted as an alternative to the sulfur point in the 1960 text of the IPTS.

---

[1] *Test fee schedules of the National Bureau of Standards (1959), available from the Office of Technical Information, NBS, Washington 25, D.C.*

[2] The International Practical Temperature Scale of 1948, *by H. F. Stimson, J. Research NBS* **65A3** *(Phys. Chem., to be published).*

[3] Temperature, its measurement and control in science and industry **1**, 141-168 (Reinhold Pub. Corp., New York, N.Y., 1941).

[4] High temperature resistance thermometry, *NBS Tech. News Bul.* **43**, *233 (Dec. 1959).*

The International Practical Temperature Scale

THE 11TH GENERAL CONFERENCE on Weights and Measures has adopted a revised text [1] of the International Temperature Scale of 1948. The new text was prepared by the National Bureau of Standards, in cooperation with other members of the Advisory Committee on Thermometry. No values of temperature on the scale have been changed, but the triple point of water (0.01 °C) has replaced the ice point as one of the six defining fixed points of the scale. To avoid confusion between the International System of Units (1954),[2] in which the unit of temperature is the degree Kelvin, and the International Temperature Scale, which is a practical scale, the name of the latter was changed to the International Practical Temperature Scale of 1948.

Although it is recognized that the Kelvin thermodynamic scale is the fundamental scale to which all temperature measurements should be referable, experimental problems make determinations on the Kelvin scale quite difficult. Therefore, in 1927, the 7th General Conference on Weights and Measures adopted an International Temperature Scale (ITS) defined by six fixed points and formulas establishing the relationship between temperature and the indications of instruments calibrated by means of the fixed points. These fixed points were the oxygen point (−182.97 °C), the ice point (0.000 °C), the steam point (100.000 °C), the sulfur point (444.6 °C), and the freezing points of silver (960.5 °C) and gold (1,063 °C). The instruments used to determine this scale are: a standard resistance thermometer over the range of −182.97 to +630.5 °C, a platinum versus platinum-10-percent-rhodium thermocouple from 630.5 to +1,063 °C, and an optical pyrometer for temperatures above 1,063 °C.

As new experimental data were accumulated, it became obvious that the ITS of 1927 would profit by revision. In 1948, therefore, three changes were adopted by the 9th General Conference. The value of the silver point was increased to 960.8 °C, Planck's radiation formula for temperatures above the gold point replaced that of Wien, and a new value for the constant C_2 used in the radiation formula was adopted. It was also decided to substitute the name Celsius [3] for that of centigrade. A recommendation was made that for work of the highest precision the triple point of water be used in place of the ice point.

Triple point cells have been in use at the Bureau for many years. Pure water is sealed in an air-free glass container, having an axial re-entrant well for the thermometer. A mantle of ice is created around the well

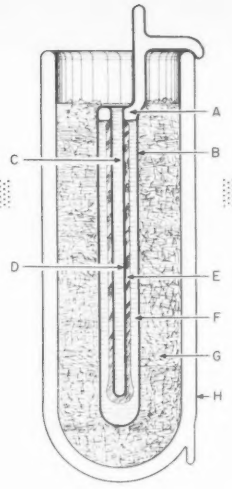

Triple point apparatus used to achieve a fixed point (0.01 °C) on the International Practical Temperature Scale. A represents water vapor; B, outer wall of the triple point cell; C, water from ice bath in re-entrant well D; E, ice mantle; F, air-free water; G, flaked ice and water; H, insulated container.

by freezing from within, and then a small amount of this mantle is re-melted to produce a water-ice interface close to the well. After a stabilizing period of a day or more, a cell kept in an ice bath is capable of maintaining a temperature constant to within 0.0001 °C for several months. The temperature at a depth, h, of immersion of the sensing element below the liquid-vapor interface is computed using the formula:

$$t = 0.01\ °C - (0.7 \times 10^{-6}\ \text{deg/mm})\ h.$$

This method is more reproducible than the procedure for realizing the ice point, which is accomplished by mixing shaved ice with air-saturated water in a Dewar flask.

In 1954 the 10th General Conference adopted a resolution redefining the Kelvin scale by assigning the value 273.16 °K to the triple point of water. This necessitated a revision of the introduction of the text of the International Temperature Scale of 1948, which stated that the interval on the Kelvin scale between the ice and steam points was 100°. The task of revision was assigned to the representative of the Bureau, who, upon reviewing the text, decided that all parts would benefit from revision. Many changes were made in the text, including the recommendation that the more reproducible temperature of freezing zinc (419.505 °C) be used in place of the boiling point of sulfur (444.600 °C) as a defining fixed point. However, it was thought that action at this time would be premature, so the sulfur point remains one of the six defining fixed points of the International Practical Temperature Scale.

The revised text was adopted by the 11th General Conference on Weights and Measures, meeting in Paris in October 1960. It includes the substitution of the triple point for the ice point as one of the defining points of the scale. Thus, the triple point, 0.01 °C or 273.16 °K, becomes the one point where the practical and thermodynamic scales exactly coincide.

---

[1] *For further technical details see* The International Practical Temperature Scale of 1948, *by H. F. Stimson, J. Research NBS* **65A** *(Phys. Chem., to be published).*

[2] *The text revision of the* International Practical Temperature Scale of 1948, *by H. F. Stimson, paper to be presented at the Fourth Symposium on Temperature, March 27–31, Columbus, Ohio.*

[3] Celsius versus centigrade, *NBS Tech. News Bul.* **33,** *110 (Sept. 1949).*

X-Ray Barrier Determinations

Measurements made by the Bureau, in a program sponsored by the Atomic Energy Commission, indicate that present methods for determining barrier requirements for X-ray installations may result in walls having protective barriers that are several half-value layers thicker than actually required.[1] This study, conducted by S. W. Smith and J. R. Brooks, with the cooperation of over 20 hospitals and clinics, may lead to savings in the cost of many future installations.

The usual procedure for the calculation of required barrier thickness is to assume near-maximum values for the various factors affecting the exposure of the barriers if more precise knowledge of them is not known. These variables include such factors as workload, fraction of time the radiation is directed toward the barrier, effect of coning, attenuation of the patient, and others. In actual practice, one or more of these factors may be considerably less than the maximum values assumed for busy installations and the barrier thickness required may thus be less than that indicated by the calculations based on these assumptions.

In this study, the amount of radiation reaching various regions of the X-ray rooms was determined through the use of pocket-type ionization chambers. As many as 70 of these instruments were attached to selected positions on the ceiling and walls of each room. Readings were taken once or twice a week, depending on the exposure, for a period of from one to two months. The penetrating quality of the radiation was determined from attenuation curves obtained from readings of instruments that were surrounded with varying thicknesses of aluminum or lead.

The work load in milliampere-minutes of each installation was automatically determined by a charge-

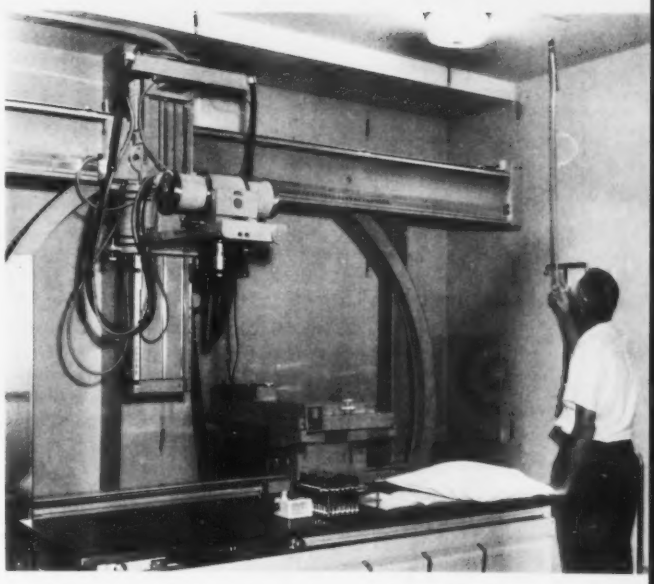

J. R. Brooks attaches pocket-type ionization chambers to the walls and ceiling of a medical X-ray room in a study of X-ray barrier requirements.

integrating device connected to the X-ray control. From the data obtained it seems reasonable to assume, when no specific information is available, a workload of 1,000 ma-min/week for a busy diagnostic X-ray room.

The amounts of lead shielding required to reduce exposure to the desired level were calculated from the collected data for those rooms having maximum exposure and use. These thicknesses were generally considerably lower than values arrived at using the usual procedure, indicating substantial safety factors.

The results of this study, combined with data from other experiments, may eventually result in a reduction in the amount of shielding specified for X-ray rooms by use of more realistic values for the various factors used in computing the barriers.

[1] *For further technical details see,* Measurement of radiation exposure at the walls of medical X-ray rooms for determining protective barrier requirements, *by S. W. Smith and J. R. Brooks, Atompraxis (March 1960).*

Hydrogen Bonding in Hydroxyapatites

THE BUREAU, in a program sponsored by the Public Health Service, has investigated the composition and structure of hydroxyapatites. A. S. Posner,[1] J. M. Stutman, and E. R. Lippincott have determined that the calcium-to-phosphorus ratio of these compounds is usually low, and that hydrogen bonds replace the missing calcium atoms.[2] This research may lead to a better understanding of the mineral portions of teeth and bones, which are also calcium-deficient apatites, and may explain the preservation of electrical neutrality in other cation-defect systems.

J. M. Stutman cks a sample of hydroxyapatite in a sapphire cell p.ior to infrared examination.

Hydroxyapatites ($Ca_{10}(PO_4)_6(OH)_2$) [3] having the stoichiometric ratio of 10Ca/6P can be formed only by using hydrothermal-bomb techniques; all of the naturally occurring apatite species are calcium deficient. Many calcium phosphates precipitated from solution give an X-ray pattern characteristic of hydroxyapatites. Analysis of these compounds, however, usually reveals that the ratio of calcium to phosphorus is low. To preserve the electrical neutrality of the system, any deficiency of calcium must be balanced by the presence of other positive ions. It was thought that hydrogen bonds might fulfill this function in hydroxyapatites, and investigation has confirmed this hypothesis.

A series of calcium-deficient hydroxyapatites were prepared by crystallization from various calcium and phosphate solutions. Each sample was examined by X-ray diffraction to make certain that only one phase was present. The amount of calcium in each sample was determined gravimetrically, and the phosphorus content was measured by differential spectrophotometry. Index of refraction measurements confirmed the X-ray and chemical evidence that the samples were calcium-deficient hydroxyapatites.

The prepared hydroxyapatites were analyzed for the presence of hydrogen bonds with an infrared spectrophotometer. Each compound exhibited an absorption

band near 3,400 cm^{-1}, which corresponds to a hydrogen-bonded O–H stretching frequency. The infrared absorption due to the hydrogen bond was found to be inversely proportional to the ratio of Ca/P. When the hydrogen bond content is zero, the pure hydroxyapatite exhibits only the O–H stretching frequency of the free hydroxyl ion near 3,700 cm^{-1}.

The general formula of hydrogen-bonded defect hydroxyapatites may be assumed to be $Ca_{10-x}H_{2x}(PO_4)_6(OH)_2$, where x has a maximum value of about 2. The hydrogen bonds are formed between oxygen atoms of adjacent orthophosphate groups. As local electrical neutrality is preserved in the crystal, it is reasonable to assume that the bonds are as near as possible to the missing columnar calcium positions. Because all of the O–H stretching frequencies fall in the 3,400 cm^{-1} range, the oxygen-oxygen distance in the hydrogen bonds does not change with different hydrogen content. The probable distance between hydrogen-bonded oxygen atoms was estimated to be 2.85 A, which agrees with the distance calculated from the atomic parameters of the crystal.

These results may be extended beyond the synthetic apatites studied in this investigation. The possible presence of hydrogen bonds in the hydroxyapatites of bone and tooth tissue may provide a basis for an estimation of the stoichiometry of these biological systems under varying conditions. Also, there are many other inorganic systems in which hydrogen bonds may compensate for the lack of certain cations.

---

[1] *Research associate of the American Dental Association Research Division at NBS.*

[2] *A. S. Posner, J. M. Stutman, E. R. Lippincott,* Hydrogen bonding in calcium deficient hydroxyapatites, *Nature* **188,** *486 (1960).*

[3] *Formulas are for unit-cell contents.*

Problem of Windstorm Damage to Asphalt Shingles

THE WIND RESISTANCE of asphalt shingle roofing, installed by different methods, has been studied at the Bureau in a project sponsored by the Air Force, the Office of the Chief of Engineers of the Army, and the Navy Bureau of Yards and Docks.

Importance of the study was pointed up by a survey conducted by the Bureau in 1958. This survey covered 54 Army, Navy, and Air Force installations from Maine to Florida, and showed that wind damage to asphalt shingle roofing had occurred at 36 installations, or 67 percent of the total. Moreover, the significance of the wind problem to civilians is emphasized by the fact that asphalt shingles constitute over 80 percent of the roofing used on sloping roofs in the United States.[1]

A guide test method for wind resistant shingles, based on results of the study, now has been adopted by the Underwriters' Laboratories, Inc., sponsored by the National Board of Fire Underwriters.

The investigation at the Bureau, conducted by William C. Cullen,[2] consisted principally of an extensive laboratory and field study of the sealing systems designed to reduce wind damage. There are two general methods of sealing the shingle tab. In one method a small amount of plastic cement is applied to the under side of each tab during installation of shingles. Under the second method, which has come into use more recently, shingles are treated with adhesive (usually asphaltic) at the time of manufacture. The shingles are then known as "self-sealing." The adhesives, placed on the under side of the shingles, seal under the influence of heat, with the exception of one type that depends upon pressure for sealing.

In actual use on buildings, solar heat accomplishes the sealing. With an ambient temperature of 90 °F, the temperature under the self-sealing shingles where the adhesive is located may be 160 °F.

The Adopted Procedure

Under the procedure adopted by Underwriters' Laboratories, the shingles being tested are subjected in the laboratory to a temperature of approximately 140 °F (under the shingle) for 16 hr. They are then required to be able to withstand a continuous wind of 60 mph for 2 hr in order to secure an acceptable rating.

As a basis for arriving at this procedure, laboratory studies had been made at the Bureau to determine the temperatures required for adequate sealing. Samples conditioned at various temperatures for 16 hr were subjected to winds of 60 mph for 2 hr. Out of 10 types, 7 sealed adequately at 140 °F, and were able to withstand the 60 mph wind for 2 hr.

Field and Laboratory Studies

The field part of the investigation showed the sealed tab shingle to be useful in windy areas. In fact, inspection of a large number of roofs in New Bern, Cherry Point, and Camp LeJeune, N.C., disclosed no failure of these materials from wind, despite widespread damage at the time of hurricane "Donna." On the other hand, inspection of unsealed shingles at the naval installation at Cherry Point, following the same hurricane, showed a loss of 2,250 squares (100 ft^2 per square) of free-tab shingles.

A related laboratory study was made of the factors that affect the wind resistance of free-tab asphalt shingles (those only nailed down, and not sealed or "locked"). This study showed that increasing the weight of the shingle, decreasing the exposure of the

Storm test machine, developed by the roofing industry, was used at the Bureau in a study of wind resistance of asphalt shingles installed by different methods. The machine can produce winds of 60 mph. Effect of the wind on the shingle is being measured by the number of inches the tab of the shingle has risen.

shingle, or increasing the weight of the felt used as the shingle base, all increase the wind resistance. Thick-butt shingles were found to be more resistant to wind than shingles of uniform thickness. Wind resistance also increases with increasing slope of the roof.

The most vulnerable area in actual use is near the ridge of the roof. Damage may be restricted to loss of a few tabs, or may result in complete loss of a roof.

A storm test machine capable of delivering a horizontal stream of air through a rectangular opening at an average velocity up to 60 mph was used in the laboratory experiments. The specimens for test consisted of asphalt shingles applied to a 4- by 3-ft plywood deck with 5-in. exposure, in accordance with standard roofing procedures. The deck was conditioned on a slope of 2 in./ft at the selected temperature for 16 hr. After conditioning, the panel was secured in the storm test machine and subjected to winds of known velocity for specific periods of time.

The amount of rise of the target tab (shingle tab in a given position relative to the orifice of the storm test machine) was used as a criterion for the wind resistance of free-tab shingles. However, the end point for failure of shingles with restrained tabs was taken as the time and wind velocity at which the restraining device failed to restrain one or more entire shingle tabs.

In an outdoor phase of the investigation, the time required for the sealing of self-sealing shingles was studied. Twenty-two samples of shingles were exposed in Washington on racks facing south on a slope of 4 in./12 in. Some shingles were white, others surfaced with dark-colored granules.

The samples were exposed in March, and inspected periodically for evidence of self-sealing. As expected, the dark-surfaced shingles sealed in the shortest time. However, after 50 days exposure, that is prior to May, the tabs of all specimens had sealed.

The adhesive bond of one tab of each sample was intentionally broken in December of the same year. By April of the following year, all tabs which had the broken bonds had resealed. The dark shingles showed better resealing ability than the white.

Inspection of 40 Roofs

In a field study, approximately 40 roofs were inspected in Florida, Louisiana, Arkansas, Texas, Northern New York, New England, and the District of Columbia. Exposure time of the shingles had varied from a few days to more than 2 yr, and the slopes on which they were applied ranged from 2 to 6 in./ft. Shingles surfaced with black, green, and white granules were observed at the various locations. Many of the roofs had been applied during cold weather and some during the summer months. Generally, the shingles were applied in wood decks over an underlayment of 15-lb asphalt-saturated felt.

In every case, performance of the self-sealing asphalt shingles appeared good. Effectiveness of the seal which occurred during outdoor exposure appeared greater than that attained by similar shingles when exposed to a temperature of 140 °F for 16 hr under controlled laboratory conditions. This may be explained in part by the fact that the sealing outdoors is a cumulative process. The process is interrupted after temperature drops—at night for example—and resumes as the roof temperature rises again. The rate of sealing is a function of both time and temperature.

Observations during the survey also confirmed previous findings that the system of sealing down the tabs of conventional asphalt shingles with a spot of plastic cement is another acceptable method for preventing wind damage.

---

[1] *J. L. Strahan*, Manufacture, selection, and application of asphalt roofing and siding products (*7th ed., rev. 1959*).

[2] *For further details see* Wind resistance of asphalt-shingle roofing, *by William C. Cullen, Proc. Bldg. Research Inst., National Research Council, 1960 Fall Conference (in process of publication).*

Measuring Resolving Power in Precision Lenses

IN AN EFFORT to reconcile discrepancies that appear in interlaboratory comparisons of lens calibrations, the Bureau recently investigated the various test patterns used to measure the resolving power of the precision lenses used in air-mapping cameras.[1] A short-line pattern of the type used in Great Britain and an annulus pattern similar to that employed in Canada were evaluated, together with a long-line pattern developed at the Bureau.[2] The evaluation showed that the best focal plane in lenses could be determined equally well with each pattern. However, no clear-cut ratio could be established between the different values for resolving power obtained with the three patterns. Data from the study may be helpful in selecting a single pattern for international use.

The highest numerical value found for the average resolving power of a lens denotes its focal plane of best average definition, and this value is used as a criterion in selecting lenses for photogrammetric purposes. In fact, a minimum acceptable value is prescribed in government specifications for precision lenses. However, considerable difficulty has been encountered in comparing lens calibration results obtained in different national standardizing laboratories. The present investigation was therefore undertaken by F. E. Washer and W. P. Tayman to evaluate the various patterns used to determine resolving power.

The equipment used to obtain data for the study consists of a precision lens-testing camera.[3] In this instrument, the lens holder is at the center of convergence of an array of 10 collimators arranged in a fan shape to cover an angle of 45°. Five charts containing the long-line patterns were used as reticles in the even-numbered collimators, and five charts each containing the other two patterns were used as reticles in the odd-numbered collimators. Thus when a negative was made of the lens under test, all three patterns could be registered on the same negative at comparable angular separations from the lens axis for the same series of focal planes in the region of usable imagery.

Test negatives made in this manner for six wide-angle lenses of the type used in air-mapping cameras were examined under a magnification of from 30 to 50. Averages of the number of lines/mm separately distinguishable in more than 200 patterns on each negative were then computed according to several different methods[4] and from these data the highest average resolving power found with each of the patterns was determined. The study showed that the long-line pattern was easiest to read and generally gave the highest values for resolving power. The short-line pattern, next easiest to read, gave the next highest values. The limit of resolution in the annulus pattern was difficult to determine, and the circular black spots in each cell of the pattern were frequently used as an aid in deciding the limit of resolution for the annulus. This pattern gave the lowest average values for resolving power. The small variations that occurred in locating the best focal plane with the three types of pattern were within the limits of experimental error.

These results indicate that resolving power is primarily a qualitative characteristic of lenses, and that its quantitative aspects should not be overemphasized. Furthermore, realistic magnitudes should be assigned to the minimum acceptable values prescribed for resolving power in establishing lens specifications.

---

[1] *For further technical details, see* Variation of resolving power and type of test patern, *by F. E. Washer and W. P. Tayman, J. Research NBS,* **64C,** *209 (1960).*

[2] Method for determining the resolving power of photographic lenses, *by F. E. Washer and I. C. Gardner NBS Circular 533 (1953), available from the Supt. of Documents, U.S. Government Printing Office, Washington 25, D.C. ($1.75).*

[3] Precision camera for testing lenses, *by I. C. Gardner and F. A. Case, J. Research NBS* **18,** *449 (1937) RP984.*

[4] Location of the plane of best average definition for airplane camera lenses, *by F. E. Washer and W. P. Tayman, Photogrammetric Engineering,* **26,** *475 (1960), and NBS Tech. News Bul.* **45,** *21 (1961).*

announcement of new publication:

Standard Frequencies and Time Signals From NBS Stations WWV and WWVH

This publication describes the six technical services broadcast by the Bureau's radio stations, WWV (Beltsville, Md.) and WWVH (Maui, Hawaii). The services include standard radiofrequencies, standard audiofrequencies, standard time intervals, standard musical pitch, time signals, and radio propagation forecasts.

Accuracy of the various services is discussed, and other topics, such as the Bureau's use of atomic frequency standards, and technical data on the radio stations—radiated power, transmitting antennas, and modulation. Also, one additional service provided by the stations is outlined—the Geophysical Alert signals. Such an alert is given to signal the occurrence of a significant magnetic storm, an outstanding auroral display, or an unusual increase in cosmic ray flux.

A separate section is included on standard frequency and time signal services provided by radio stations other than WWV and WWVH.

Standard Frequencies and Time Signals From NBS Stations WWV and WWVH, NBS Miscellaneous Publication 236, issued Dec. 1, 1960, 6 pages, 10 cents. (Order from the Superintendent of Documents, U.S. Government Printing Office, Washington 25, D.C.)

Publications of the National Bureau of Standards

Periodicals

Technical News Bulletin, Volume **45**, No. 3, March 1961. 15 cents. Annual subscription: $1.50, 75 cents additional for foreign mailing. Available on a 1-, 2-, or 3-year subscription basis.

Basic Radio Propagation Predictions for June 1961. Three months in advance. CRPL–D199, issued March 1961. 15 cents. Annual subscription $1.50, 50 cents additional for foreign mailing. Available on a 1-, 2-, or 3-year subscription basis.

Journal of Research of the National Bureau of Standards

Section A. Physics and Chemistry. Issued six times a year. Annual subscription: Domestic, $4; foreign, $4.75.

Section B. Mathematics and Mathematical Physics. Issued quarterly. Annual subscription: Domestic, $2.25; foreign $2.75.

Section C. Engineering and Instrumentation. Issued quarterly. Annual subscription: Domestic, $2.25; foreign, $2.75.

Section D. Radio Propagation. Issued six times a year. Annual subscription: Domestic, $4; foreign, $4.75.

Section D. Radio Propagation, Volume **65D**, No. 2, March-April 1961.

Ionospheric motions observed with high-frequency backscatter sounders. L. H. Tveten.

Relationship between red auroral arcs and ionospheric recombination. G. A. M. King and F. E. Roach.

Fresnel region fields of circular aperture antennas. Ming-Kuei Hu.

Free-balloon borne meteorological refractometer. John F. Theisen and Earl E. Gossard.

Weather and reception level on a troposphere link—annual and short-term correlations. L. G. Abraham, Jr., and J. A. Bradshaw.

Initial results of a new technique for investigating sferic activity. Gifford Hefley, Robert H. Doherty, and Robert F. Linfield.

Effect of antenna radiation angles upon HF radio signals propagated over long distances. W. F. Utlaut.

Graphic determination of radio ray bending in an exponential atmosphere. C. F. Pappas, L. E. Vogler, and P. L. Rice.

A formula for radio ray refraction in an exponential atmosphere. G. D. Thayer.

The impedance of a monopole antenna with a circular conducting-disk ground system on the surface of a lossy half-space. S. W. Maley and R. J. King.

Radio-wave propagation in the earth's crust. Harold A. Wheeler.

Nonperiodicals

Measurement of absorbed dose of neutrons, and of mixtures of neutrons and gamma rays. NBS Handb. H75 (1961) 35 cents.

Medical X-ray protection up to three million volts. NBS Handb. H76 (1961) 25 cents.

Precision measurement and calibration, S. F. Booth: Electricity and electronics, NBS Handb. 77, Vol. I (1961) $6.00; Heat and mechanics, NBS Handb. 77, Vol. II (1961) $6.75; Optics, metrology, and radiation, NBS Handb. 77, Vol. III (1961) $7.00.

Publications in Other Journals

Regulated power supply for instruments, W. V. Loebenstein, Electronics **33**, No. 48, 132 (Nov. 1960).

Effect of structure on the spectra emitted by solid nitrogen during electron bombardment, L. J. Schoen and H. P. Broida, J. Mol. Spectroscopy **5**, No. 5, 416–419 (Nov. 1960).

Chemical reactions of free radicals at low temperatures, R. A. Ruehrwein, J. S. Hashman, and J. W. Edwards, J. Phys. Chem. **64**, 1317–1322 (1960).

Experimental investigation of creep deflection of extruded and riveted I-beams, L. Mordfin and N. Halsey, NASA Tech. Note D-662 (Dec. 1960).

Spatial distribution of energy dissipated by fallout β-rays, A. E. Boyd and E. E. Morris, Health Phys. **2**, 321–325 (1959).

Megaroentgen dosimetry employing photographic film without processing, W. L. McLaughlin, Radiation Research **13**, No. 4, 594–609 (Oct. 1960).

The reaction of hydrogen atoms with solid propene at low temperatures, R. Klein, M. D. Scheer and J. G. Waller, J. Phys. Chem. **64**, 1247–1250 (1960).

The measurement of thermal conductivity, D. C. Ginnings, Book, Thermoelectric Materials and Devices, edited by I. B. Cadoff and E. Miller. Ch. 8, 113–132 (Reinhold Publ. Corp., New York, N.Y., 1960).

Programming for a closed-loop, manned-machine combined system, D. C. Friedman, Proc. Combined Analog-Digital Computer Systems Symp., December 16 and 17, 1960, Philadelphia, Pa., 12th Article (Dec. 1960).

Irrational power series, M. Newman, Proc. Am. Math. Soc. **11**, 699–702 (Oct. 1960).

Analytical study of creep deflection of structural beams, L. Mordfin, NASA Tech. Note D-661 (Dec. 1960).

Evaluation of ball bearing separator materials operating submerged in liquid nitrogen, W. A. Wilson, K. B. Martin, J. A. Brennan, and B. W. Birmingham, ASLE, ASME Lubrication Conf., October 17–19, 1960 (Boston, Mass.), Am. Soc. Lubrication Engrs. Preprint No. 60 LC–4 (1960).

Microwave spectrum, structure, and dipole moment of propane, D. R. Lide, Jr., J. Chem. Phys. **33**, No. 5, 1514–1518 (Nov. 1960).

Topological derivation of the Mayer density series for the pressure of an imperfect gas, M. S. Green, J. Math. Phys. **1**, No. 5, 391–394 (Sept.–Oct. 1960).

Surface area determination of kaolinite using glycerol adsorption, K. H. Woodside and W. C. Ormsby, J. Am. Ceram. Soc. **43**, No. 12, 671–672 (Dec. 1960).

Magnetic resonance determination of the nuclear moment of tantalum-181 in $KTaO_3$, L. H. Bennett and J. I. Budnick, Phys. Rev. **120**, No. 5, 1812–1815 (Dec. 1, 1960).

Aircraft storage batteries, W. J. Hamer, AIEE Trans. **79**, Pt. II, 1–11 (Sept. 1960).

Electrodeless passage of direct current through an electrolyte, A. Brenner, J. Electrochem. Soc. **107**, No. 12, 968–973 (Dec. 1960).

Preparation and thermal stability of tetrakis-(pentafluorophenyl)-silane and tris-(pentafluorophenyl)-phosphine, L. A. Wall, R. E. Donadio, and W. J. Pummer, J. Am. Chem. Soc. **82**, No. 18, 4846–4852 (Sept. 1960).

Stress-strain relationships in yarns subjected to rapid impact loading. Part VI: Velocities of strain waves resulting from impact, J. C. Smith, J. M. Blandford, and H. F. Schiefer, Textile Research J. **30**, No. 10, 752–760 (Oct. 1960).

The centennial of spectrochemistry, W. F. Meggers and J. L. Tech, J. Opt. Soc. Am. **50**, No. 11, 1035–1038 (Nov. 1960).

Rate of reaction of nitrogen atoms with ethylene, J. T. Herron, J. Chem. Phys. **33**, No. 4, 1273–1274 (Oct. 1960).

Structure of the isobutane molecule; change of dipole moment on isotopic substitution, D. R. Lide, Jr., J. Chem. Phys. **33**, No. 5, 1519–1522 (Nov. 1960).

Condensation coefficient of arsenic trioxide glass, A. B. Bestul and D. H. Blackburn, J. Chem. Phys. **33**, No. 4, 1274–1275 (Oct. 1960).

The compound $BaTiGe_2O_6$, C. R. Robbins, J. Am. Ceram. Soc. **43**, No. 11, 610 (Nov. 1960).

The relation of $h_{max}F2$ to $M(3000)F2$ and H_pF2, J. W. Wright and R. E. McDuffie, J. Radio Research Lab. **7**, No. 32, 409–420 (July, 1960).

8-quinolinol precipitation of the elements, J. I. Hoffman, Chem. Anal. **49**, No. 4, 126 (Dec., 1960).

Dipole moments of hydrocarbons, D. R. Lide, Jr., J. Chem. Phys. **33**, No. 6, 1879 (Dec., 1960).

Collection of ions produced by alpha particles in air, Z. Bay and H. H. Seliger, Phys. Rev. **120**, No. 1, 141–143 (Oct 1, 1960).

UNITED STATES
GOVERNMENT PRINTING OFFICE
DIVISION OF PUBLIC DOCUMENTS
WASHINGTON 25, D.C.

OFFICIAL BUSINESS

PENALTY FOR PRIVATE USE TO AVOID
PAYMENT OF POSTAGE, $300
(GPO)

Publications (*Continued*)

A test of a procedure for easy estimation of representative monthly electron density profiles for the ionosphere, J. W. Wright, J. Geophys. Research **65,** No. 10, 3215–3217 (Oct., 1960).

A method for efficiently providing low temperature liquids on a large scale to an accelerated experimental program, A. K. Stober, Proc. 10th Intern. Congress of Refrigeration, Copenhagen, Denmark **1,** No. 1, 17–18 (Pergamon Press Ltd., London, England, 1959).

Seasonal variations in the twilight enhancement of [OI] 5577, L. R. Megill, P. M. Jamnick and J. E. Cruz, J. Atmospheric and Terrest. Phys. **18,** 309–314 (Aug., 1960).

Synthetic mica, A. Van Valkenburg, Book, Encyclopedia of Chemical Technology, p. 480–487 (Interscience Encyclopedia, Inc., New York, N.Y., 1960).

Nonresonant microwave absorption and relaxation frequency at elevated pressures, A. A. Maryott and G. Birnbaum, J. Phys. Chem. **64,** No. 11, 1778–1780 (Nov., 1960).

Precipitation of the elements on addition of aqueous ammonia to their clear solution, J. I. Hoffman, Chem.-Anal. **49,** No. 3, 94 (Sept., 1960).

Low scatter high current gas target for D–D neutrons, A. C. B. Richardson, Rev. Sci. Inst. **31,** No. 11, 1202–1203 (Nov., 1960).

The heat of combustion of dicyanoacetylene, G. T. Armstrong and S. Marantz, J. Phys. Chem. **64,** 1776–1777 (1960).

Evaluation of resistance strain gages at elevated temperatures, R. L. Bloss, Am. Soc. Testing Materials Proc. **1,** No. 1, 9–15 (Jan., 1961).

Errors in dielectric measurements due to a sample insertion hole in a cavity, A. J. Estine and H. E. Bussey, IRE Trans. Microwave Theory and Tech. **MTT–8,** No. 6, 650–653 (Nov., 1960).

Ensemble method in the theory of irreversibility, R. Zwanzig, J. Chem. Phys. **33,** No. 5, 1338–1341 (Nov., 1960).

Determination of pentosans. Interlaboratory comparison of the aniline acetate, orcinol, and bromination methods, W. K. Wilson and J. Mandel, Tappi **43,** No. 12, 998–1004 (Dec., 1960).

A research for geomagnetic singular days, C. Warwick, T. Pohrte, and N. MacDonald, J. Geophys. Research **65,** No. 9, 3013–3015 (Sept., 1960).

Letter to editor of Revue des Matériaux (first), E. S. Newman and H. A. Berman, Revue des Matériaux **C,** No. 540, 231 (Dec. 1, 1960).

Geomagnetic storms and the space around the earth, S. Chapman, Nature **187,** No. 4740, 824–827 (Sept. 3, 1960).

On the theory of the critical point of a simple fluid, M. S. Green, J. Chem. Phys. **33,** No. 5, 1403–1409 (Nov., 1960).

Some implications of slant-E_s, E. K. Smith and R. W. Knecht, Polar Atmosphere Symp., Part 2, Ionospheric Section, Oslo, Norway, July 2–8, 1956, p. 195–204 (Pergamon Press, Inc., New York, N.Y., 1957).

Mismatch errors in microwave phase shift measurements, G. E. Schafer, IRE Trans. Microwave Theory and Tech. **MTT–8,** No. 6, 617–622 (Nov. 1960).

Residual arc spectra of seventy elements diluted in copper, C. H. Corliss, W. F. Meggers and B. F. Scribner, Book, Colloquium Spectroscopicum Internationale VIII, 119–121 (1959).

The rotational constants of hydrogen chloride, E. K. Plyler and E. D. Tidwell, Z. Elektrochem. **64,** No. 5, 717–720 (Feb. 1960).

Publications for which a price is indicated (except for Technical Notes) are available only from the Superintendent of Documents, U.S. Government Printing Office, Washington 25, D.C. (foreign postage, one-fourth additional). Reprints from outside journals and the NBS Journal of Research may often be obtained directly from the authors.

Equations Representing Steel Expansion

THE BUREAU has developed a set of equations to represent the thermal expansion of mild steel from −40 to +400 °F, at the request of the American Society for Testing Materials. These equations were derived to assist ASTM Committee D–2 on Petroleum Products and Lubricants in the development of steel standards involving volume. They may also be used in preparing specifications for the steel containers used for storing various types of petroleum products.

To make these equations generally available, they are published here:

$$L_t = L_{60}[1 + 6.2\times10^{-6}(t-60) + 2.0\times10^{-9}(t-60)^2]$$

$$\alpha_m = [6.0\times10^{-6} + 2.0\times10^{-9}(t_1+t_2)]/°\text{F}$$

$$V_t = V_{60}[1 + 18.6\times10^{-6}(t-60) + 6.1\times10^{-9}(t-60)^2]$$

$$\beta_m = [17.9\times10^{-6} + 6.1\times10^{-9}(t_1+t_2)]/°\text{F}$$

where L_t and L_{60} are the lengths at temperatures t and 60 °F; α_m is the mean or average coefficient of linear expansion per degree Fahrenheit between temperatures t_1 and t_2; V_t and V_{60} are the volumes and β_m is the mean or average coefficient of cubical expansion per degree Fahrenheit.

The values used in these equations are believed to be representative for mild steels to the accuracy of the digits given.

U.S. GOVERNMENT PRINTING OFFICE: 1961 O—587453